Equilibrium Electric Double Layer of Charged Spherical Colloidal Particles: Effect of Different Distances of Minimum Ion Approach to The Particle Surface

J. J. López-García,[†] M. J. Aranda-Rascón,[†] C. Grosse,[‡,§] and J. Horno*[,†]

Departamento de Física, Universidad de Jaén, Campus Las Lagunillas, Ed. A-3, 23071, Jaén, Spain, Departamento de Física, Universidad Nacional de Tucumán, Avenida Independencia 1800, 4000 San Miguel de Tucumán, Argentina, and Consejo Nacional de Investigaciones Científicas y Técnicas, Avenida Rivadavia 1917, 1033 Buenos Aires, Argentina

Received: December 29, 2009; Revised Manuscript Received: April 20, 2010

A study of the equilibrium double layer surrounding charged spherical particles is presented, considering that ions in the suspending medium have a finite size. It is assumed that each ionic species has a different minimum approach distance to the particle surface, while the distance of minimum approach between ions in the bulk has the same value for all ion species. Numerical calculations made using the network simulation method and including all the features of the considered model are presented, together with rigorous analytical results valid for a flat interface and point ions in the bulk electrolyte solution. It is shown that the double-layer parameters are very sensitive to the difference between the minimum approach distances of co-ions and counterions. For negative particles and greater approach distances for co-ions than for counterions, the potential always increases with this difference and, under appropriate circumstances, attains positive values leading to charge reversal. This phenomenon is favored by a high electrolyte concentration, high counterion valences, and low surface charge (in modulus). An analytical expression relating these parameters to the threshold value of the difference between the minimum approach distances of co-ions and counterions to the particle surface is presented.

Introduction

The existence of an electrical double layer surrounding dispersed colloidal particles has a profound effect on a wide variety of both equilibrium and nonequilibrium phenomena in colloidal science. This is the reason for the great importance and interest in models of the double layer. While the theoretical model based on the Poisson−Boltzmann equation is an acknowledged and widely used description of the diffuse part of the equilibrium double layer,[1−3] it is based on a series of simplifying assumptions: the finite sizes of ions are neglected; non-Coulombic interactions between counterions, co-ions, and the particle surface are disregarded; the permittivity of the medium is assumed to be constant; incomplete dissociation of the electrolyte is ignored; and so forth. In particular, the consideration of ions as mathematical points has fundamental consequences on the behavior of the equilibrium double layer surrounding charged suspended particles.

The early attempts made to challenge this assumption[4−8] generally concluded that the finite size of ions has an almost negligible effect except for particles with an extremely high surface charge so that, in most cases of practical interest, ions do indeed behave as point charges. This subject has regained interest in later years because of the advent of computational methods that made it possible to numerically solve the complex equations involving finite ion size. Roughly, two types of methods have been used to include ion interactions into the theoretical model: microscopic descriptions of the system with different approach levels[9−15] and phenomenological theories using macroscopic differential equations to describe the behavior of the system.[16−29] Microscopic descriptions have the advantage of precisely representing the interactions responsible for the macroscopic behavior of the system, but only in equilibrium. On the contrary, phenomenological theories, less strict in the description of the interactions, make it possible to analyze the system behavior both in equilibrium and perturbed by an external signal.[23,25−27,29] (See the review of Bazant et al.[29] for a historical background.)

In a series of works[24−27] we have shown that excluded volume can have a marked effect on the dielectric an electrokinetic properties of colloidal suspensions even for typical surface charge values. There are two main reasons for this qualitative discrepancy between our conclusions and those of earlier works. The first is that a finite ion size not only determines a minimum approach distance between ions in the bulk electrolyte solution but also determines a minimum approach distance between ions and the particle surface. The second is that classical works only studied the finite ion size effects on the equilibrium electric potential and ion concentration distributions, while the dielectric and electrokinetic properties are nonequilibrium phenomena. We have shown that the largest changes occur in the field-induced convective flows that are strongly dependent on the minimum approach distance between ions and the particle surface.

In our preceding works, we considered that all the ion species have the same size, and that this size determines the minimum approach distance both between ions in the bulk electrolyte solution and between ions and the particle surface. While this is the simplest assumption, it does not necessarily provide the best representation of the real situation, as recognized since the classic 1947 work of Grahame.[30] Ion size is not a simple geometrical parameter: it is not only determined by the steric ion volume but also by the possible existence of a hydration shell and by the ion−ion or ion−particle surface interaction. These two types of interactions are generally different, which

* Corresponding author: E-mail address: jhorno@ujaen.es.
[†] Universidad de Jaén.
[‡] Universidad Nacional de Tucumán.
[§] Consejo Nacional de Investigaciones Científicas y Técnicas.

10.1021/jp9122369
Published on Web 05/17/2010

leads to the possibility that ions having the same effective size have, nevertheless, different values of the minimum approach distance to the particle surface. In the present work we explore this possibility and its influence on the structure of the equilibrium diffuse double layer. We show that, for reasonable parameter values, important quantitative changes are to be expected. Furthermore, under favorable circumstances, a qualitative change should occur: the charge reversal phenomenon.

Theory

Let us consider a charged spherical particle of radius a immersed in an unbounded electrolyte solution. The starting point of our study will be the Poisson equation relating the electric potential, $\phi(r)$, to the volume charge density, $\rho(r)$, at any point of the system. Its expression in spherical coordinates with spherical symmetry is

$$\frac{1}{r^2}\frac{\mathrm{d}}{\mathrm{d}r}\left[r^2\frac{\mathrm{d}\phi(r)}{\mathrm{d}r}\right] = -\frac{\rho(r)}{\varepsilon_e} = -\frac{eN_A}{\varepsilon_e}\sum_{i=1}^{m} z_i c_i(r) \qquad (1)$$

where z_i and $c_i(r)$ are the signed valence and the local concentration (in moles per unit volume) of the ionic species i ($i = 1, ..., m$), e is the elementary charge, N_A is the Avogadro number, and ε_e is the dielectric permittivity of the solution, which is assumed to have a constant value for $r > a$.

In the bulk solution far from the particle surface, each ion occupies an effective volume due to its finite size and to the ion−ion interactions, so that the local concentration of each ionic species is limited by a maximum concentration, c_i^{max}. This limiting local concentration behavior can be expressed by means of a Langmuir type function:[6−25]

$$c_i(r) = \frac{K_i \exp\left[-\frac{z_i e\phi(r)}{kT}\right]}{1 + \sum_{i=1}^{m}\frac{K_i}{c_i^{max}}\left\{\exp\left[-\frac{z_i e\phi(r)}{kT}\right] - 1\right\}} \qquad (2)$$

where K_i are integration constants (Appendix A), which are generally different for each ionic species. Their values are equal to the value of the ionic concentrations at spatial points where the electric potential is zero. In particular, assuming the potential origin at $r \to \infty$, K_i take the values of the bulk concentrations c_i^{∞}. Note that the usual form of the Poisson−Boltzmann equation for a spherical double layer is obtained from eqs 1 and 2 assuming that $c_i^{max} \to \infty$ (ideal ion behavior). Moreover, assuming a simple cubic structure, a value for the effective ionic radius can be calculated from the value of c_i^{max}:[25]

$$R_i = \frac{1}{\sqrt[3]{8N_A c_i^{max}}} \qquad (3)$$

On the other hand, due to the finite ionic size and to the ion−particle surface interaction, we assume that ions of species i cannot come closer to the particle surface than an effective distance of minimum approach h_i. The simplest way to take this effect into account is to consider that, for the region $a < r < a + h_i$, the concentration of the ionic species i vanishes. This implies that the constant K_i is equal to zero in this region.[27]

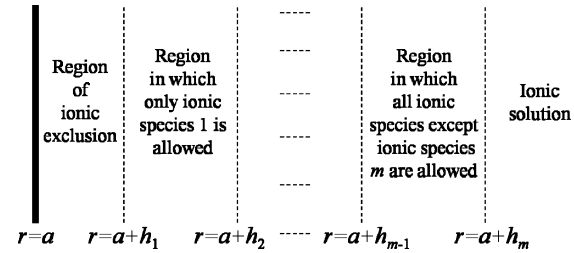

Figure 1. Graphical representation of the different layers considered in the theoretical model.

In previous works,[26,27] we considered that the minimum approach distance to the particle surface of each ionic species, h_i, is equal to the corresponding effective ionic radius, R_i. Accordingly, the consideration of different effective ionic sizes should lead to different minimum approach distance values for each ionic species. However, it is reasonable to assume that, since the values of h_i depend on the ion−particle surface interaction, even ionic species with the same effective volume in the solution could have different minimum approach distances to the particle surface.

In this work we consider that all the ionic species have different minimum approach distances and that they are ordered in such a way that $h_i \le h_{i+1}$ for $i = (1, 2, ..., m - 1)$. Therefore, the region next to the particle surface can be divided into a series of layers as shown in Figure 1. As already noted, the constants K_i of the ionic concentrations are zero for $a < r < a + h_i$ and equal to the bulk concentration of the ionic species c_i^{∞}, for $a + h_i < r$ (Appendix A).

Combining eqs 1 and 2, the generalized Poisson equation becomes

$$\frac{1}{r^2}\frac{\mathrm{d}}{\mathrm{d}r}\left[r^2\frac{\mathrm{d}\phi(r)}{\mathrm{d}r}\right] = -\frac{eN_A}{\varepsilon_e}\frac{\sum_{i=1}^{m} z_i K_i \exp\left[-\frac{z_i e\phi(r)}{kT}\right]}{1 + \sum_{i=1}^{m}\frac{K_i}{c_i^{max}}\left\{\exp\left[-\frac{z_i e\phi(r)}{kT}\right] - 1\right\}} \qquad (4)$$

where

$$K_i = \begin{cases} 0 & a < r < a + h_i \\ c_i^{\infty} & a + h_i < r \end{cases} \qquad (5)$$

The boundary conditions needed to solve eq 4 are

$$\phi(a) = \phi_s \qquad (6)$$

$$\left.\frac{\mathrm{d}\phi(r)}{\mathrm{d}r}\right|_{r=a} = -\frac{\sigma_s}{\varepsilon_e} \qquad (7)$$

$$\phi((a + h_i)^-) = \phi((a + h_i)^+) \qquad (8)$$

$$\left.\frac{\mathrm{d}\phi(r)}{\mathrm{d}r}\right|_{r=(a + h_i)^-} = \left.\frac{\mathrm{d}\phi(r)}{\mathrm{d}r}\right|_{r=(a + h_i)^+} \qquad (9)$$

$$\left.\frac{\mathrm{d}\phi(r)}{\mathrm{d}r}\right|_{r\to\infty} \to 0 \qquad (10)$$

Boundary condition 6 implies the knowledge of the electric potential value at the particle surface; 7 is the Gauss law relating

the surface charge density of the particle σ_s to the normal component of the electric field at its surface; 8 and 9 express the continuity of the electric potential and of the normal component of the electric displacement at the boundaries between the different regions of the system; and 10 specifies the global electroneutrality of the system. Note that the choice of boundary conditions 6 or 7 depends on the knowledge of either the surface potential or the surface charge of the particle. These two conditions cannot be simultaneously used.

It is usual to use the variables

$$y(r) = \frac{e\phi(r)}{kT} \tag{11}$$

$$x = r - a \tag{12}$$

which transform eq 4 into

$$\frac{d^2y(x)}{dx^2} + \frac{2}{x+a}\frac{dy(x)}{dx} = -\frac{e^2N_A}{kT\varepsilon_e}\frac{\sum_{i=1}^{m} z_iK_i \exp[-z_iy(x)]}{1 + \sum_{i=1}^{m}\frac{K_i}{c_i^{max}}\{\exp[-z_iy(x)] - 1\}} \tag{13}$$

while the boundary conditions, eqs 6−10, become

$$y(0) = \frac{e\phi_s}{kT} = y_s \tag{14}$$

$$\left.\frac{dy(x)}{dx}\right|_{x=0} = -\frac{e\sigma_S}{\varepsilon_e kT} \tag{15}$$

$$y(h_i^-) = y(h_i^+) \tag{16}$$

$$\left.\frac{dy(x)}{dx}\right|_{x=h_i^-} = \left.\frac{dy(x)}{dx}\right|_{x=h_i^+} \tag{17}$$

$$\left.\frac{dy(x)}{dx}\right|_{x\to\infty} \to 0 \tag{18}$$

Note that the theoretical model presented here reduces to the theoretical models presented in ref 27 for $h_i = R_i = R\ \forall i \in (1, ..., m)$, to the model used in ref 25 for $h_i = 0\ \forall i \in (1, ..., m)$, and to the classical model (Poisson−Boltzmann equation) for $h_i = 0$ and $c_i^{max} \to \infty\ \forall i \in (1, ..., m)$.

Numerical Calculations. There is no general analytical solution for the theoretical model presented above. Only for the case of plane geometry ($a \to \infty$) and of point ions ($c_i^{max} \to \infty$), analytical solutions exist (see Appendix B). Therefore, numerical methods are necessary to solve the model in the general case.

The numerical calculations were performed using an algorithm based on the network simulation method, which consists of modeling the governing differential equations by means of an electrical circuit. A full account of the network model used in this work is given in refs 31 and 32, and a more general explanation of the method is given in ref 33.

It must be noted that, since the electric potential changes rapidly near the interface $x = 0$, an appropriate simulation space grid must be modeled. In this work, the x-space grid is automatically adapted to the evolution of the electric potential profiles. If, in the course of the simulation, strong changes of y with x are detected in any x coordinate region, more grid points are added into that region. Appropriate simulation space grids were calculated in this way to ensure good accuracy and moderate CPU times.

Results

Except when indicated otherwise, the simulations were made using the parameter values shown in Table 1.

We consider the particular case of a negative surface charge value because colloidal particles suspended in aqueous electrolyte solutions usually acquire a negative charge. Therefore, counterions are positive (cations) while co-ions are negative (anions). For simplicity, we also assume that there are only two ion species in the electrolyte solution.

It was shown in the literature[36] that the typical value of the effective ionic solvated diameter, determined from mobility measurements, is approximately 0.6−0.8 nm. However, the effective ion size to be used in the considered theoretical model should be larger due to the ion−ion interactions.[29] The value of c_i^{max} for the two ionic species was chosen considering an effective solvated diameter in water of approximately 1 nm. On the other hand, the minimum approach distance to the particle surface has been chosen as equal to 0.5 nm for counterions and 1.5 nm for co-ions. This corresponds to the assumption that co-ions are excluded from the first monolayer of counterions.[22] Note that our hypothesis does not coincide with the classical Grahame model,[30] which assumes that the minimum approach distance of counterions is smaller than that of co-ions because the effective radius of adsorbed counterions in the first monolayer is smaller than in the bulk.

Our assumptions could be compared to those used in existing hard sphere simulations:[34,35] the treatment of the excluded volume effect is analogous to the local density approximation while the incorporation of different minimum approach distances of co-ions and counterions might be regarded as a weighted density approximation for the nonlocal correlations between ions and the surface. These studies generally show that the local density approximation does not suffice for a good representation of the double layer properties that require the use of weighted density approximations.

In what follows, we present numerical results for the dimensionless potential, y, as a function of the distance to the particle surface, x, for different situations of interest. Once the potential−distance relationship is solved, it is immediate to obtain the ionic concentrations at any point of the double layer using eq 2.

Figure 2 shows the dependence of the electric potential and the ion concentration profiles on the difference between the minimum approach distances of co-ions and counterions. As can be observed, these profiles are generally similar to those corresponding to equal minimum approach distances previously analyzed.[26] However, the following important differences should be noted:

TABLE 1

$\sigma_S = -0.02$ C/m^2	$a = 100$ nm	$z = z_1 = -z_2 = 1$
$c_1^\infty = 100$ mol/m^3	$h_1 = 0.5$ nm	$c_1^{max} = 1500$ mol/m^3
$c_2^\infty = 100$ mol/m^3	$h_2 = 1.5$ nm	$c_2^{max} = 1500$ mol/m^3
$T = 298$ K	$\varepsilon_e = 78.54\cdot\varepsilon_0$	$\varepsilon_0 = 8.854\ 10^{-12}$ F/m
$k = 1.381\ 10^{-23}$ J/K	$N_A = 6.022\ 10^{23}$ mol^{-1}	$e = 1.602\ 10^{-19}$ C

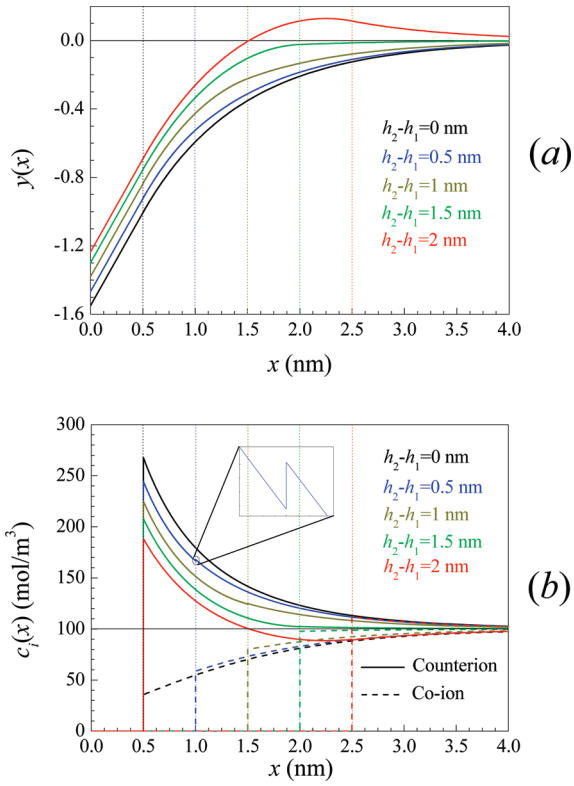

Figure 2. (a) Dimensionless electric potential and (b) ion concentration profiles for the indicated differences between the minimum approach distances to the particle surface of co-ions and counterions. The remaining parameters are given in Table 1.

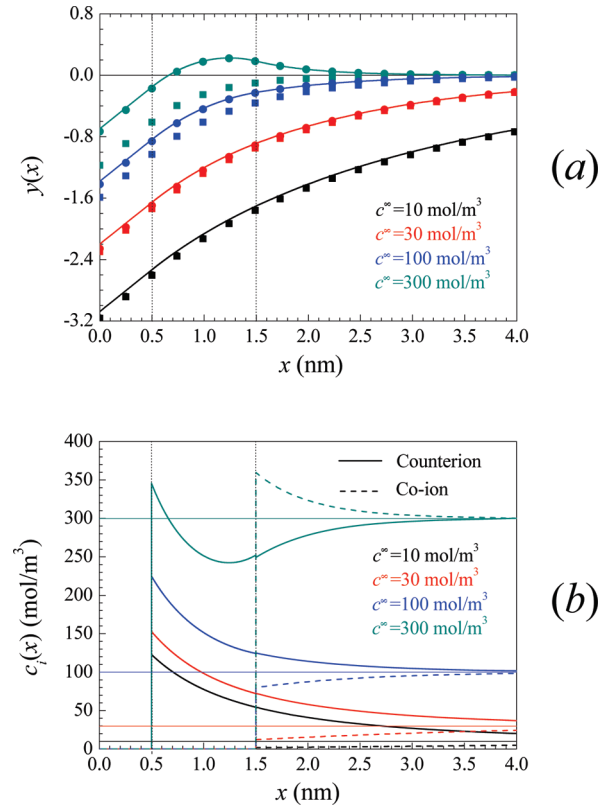

Figure 3. (a) Dimensionless electric potential and (b) ion concentration profiles for the indicated bulk ion concentrations. The symbols represent analytical results (Appendix B) corresponding to a plane interface, $c_i^{max} \rightarrow \infty$, and either the same h_1 and h_2 values as used in the numerical simulation (circles) or $h_1 = h_2 = 0.5$ nm (squares). The remaining parameters are given in Table 1.

(a) The surface potential as well as the potential at all points around the particle increases when the difference between the minimum approach distances of co-ions and counterions, $h_2 - h_1$, increases while h_1 is kept at a constant value. When the minimum approach distance of co-ions increases, the region accessible to only positive counterions increases, so that the electric charge inside a sphere of radius r also increases, which leads to higher values of the electric potential.

(b) The co-ion concentration vanishes in the $0 < x < h_2$ region, and its value at $x = h_2$ increases when h_2 increases. An increase of h_2 leads to a corresponding increase of the electric potential (preceding point) and, therefore, to a smaller co-ion concentration deviation with respect to its bulk value.

(c) The counterion concentration at $h_2 < x$ decreases when h_2 increases. Just as in the preceding point, an increase of the electric potential leads to a lower deviation of the counterion concentration relative to its bulk value.

(d) The counterion concentration profiles are discontinuous at $x = h_2$ because of the discontinuity of the co-ion concentration (eqs 2 and 4).

(e) For sufficiently large values of the difference $h_2 - h_1$, the total electric charge of counterions in the $h_1 < x < h_2$ layer surpasses the absolute value of the electric charge of the particle, leading to charge reversal. Thus, for $h_2 < x$, positive ions behave as co-ions and negative ions behave as counterions. This charge reversal phenomenon due to ionic size has been analyzed in several works using Monte Carlo simulations[10−14] and in a recent theoretical prediction based on the Poisson−Boltzmann equation.[21]

Figure 3 shows the dependence of the electric potential and the ion concentration profiles on the bulk ion concentration. In Figure 3a, analytical results (Appendix B) have been included for comparison. These results correspond to the cases of a plane interface and $c_i^{max} \rightarrow \infty$ (circles) and to a plane interface, $c_i^{max} \rightarrow \infty$, and $h_1 = h_2 = 0.5$ nm (squares). Horizontal lines indicating the bulk concentrations for the considered cases, have been included in Figure 3b. The following important features can be observed in this figure:

(a) As expected, the surface potential increases in absolute value when the bulk concentration decreases. This effect is due to the dependence of the thickness of the diffuse double layer with the electrolyte concentration: the Debye length defined as

$$\kappa^{-1} = \sqrt{\frac{kT\varepsilon_e}{e^2 N_A \sum_{i=1}^{m} z_i^2 c_i^\infty}} \qquad (19)$$

increases when the ion concentrations are lowered.

(b) In the case where $c_i^\infty = 300$ mol/m^3, the counterion concentration in the $h_1 < x < h_2$ region becomes so high that the electric charge of the particle is completely shielded, leading to charge reversal.

(c) The analytical solution for a plane interface, $c_i^{max} \rightarrow \infty$, and the same minimum approach distance values as in the numerical simulation (circles), leads to results that are very close to the numerical ones. However, small deviations become apparent at the lowest concentrations when the assumption of a plane interface becomes

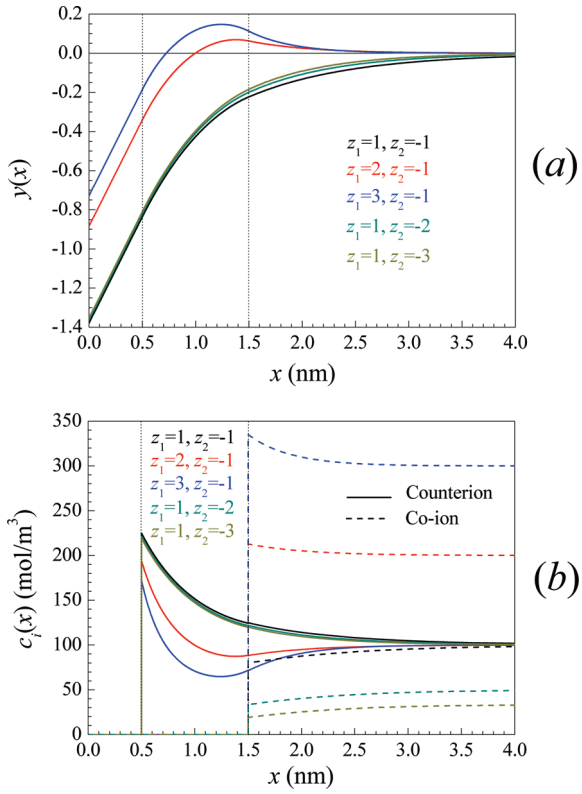

Figure 4. (a) Dimensionless electric potential and (b) ion concentration profiles for the indicated counterion and co-ion valences. The remaining parameters are given in Table 1, except for the co-ion concentration that varies while the counterion concentration $c_1^\infty = 100$ mol/m^3 remains constant.

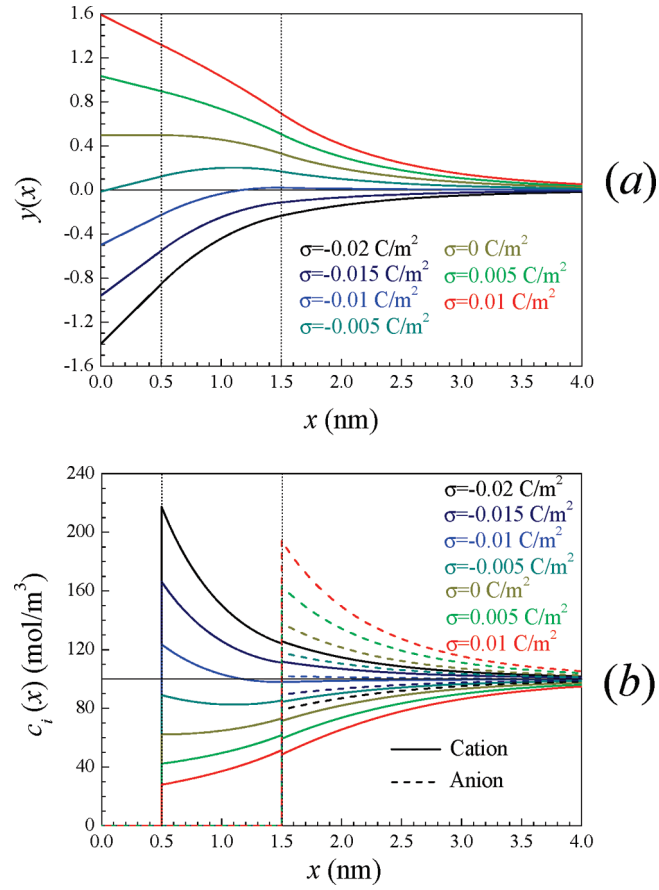

Figure 5. (a) Dimensionless electric potential and (b) ion concentration profiles for the indicated surface charge values. The remaining parameters are given in Table 1.

objectionable. Actually, analytical results have not been included in the remaining figures because they are indistinguishable from the numerical ones for the parameter values given in Table 1.

(d) The analytical solution for a plane interface, $c_i^{max} \to \infty$, and $h_1 = h_2 = 0.5$ nm (squares), leads to results that are only acceptable for low electrolyte concentrations. Under these conditions, the electric potential close to the particle is large (in absolute value) so that the co-ion concentration is very low. Therefore, the presence of an exclusion region for co-ions has little bearing on the potential profiles. On the contrary, the presence of this region becomes all important at high electrolyte concentrations and correspondingly low absolute potential values. The high concentration of co-ions close to the particle lowers the concentration of counterions and eliminates the possibility of charge reversal.

The analytical solution given in Appendix B makes it possible to derive the following condition for the occurrence of charge reversal:

$$h_2 - h_1 > \frac{1}{z_1 e}\sqrt{\frac{2kT\varepsilon_e}{c_1^\infty N_A}}\tan^{-1}\sqrt{\frac{\sigma_s^2}{2kT\varepsilon_e c_1^\infty N_A}} \qquad (20)$$

As can be seen, this expression predicts that an increase of the bulk concentration facilitates charge reversal, in agreement with Figure 3. Furthermore, according to eq 20, an increase of the counterion valence should also facilitate this phenomenon. This effect can be observed in Figure 4, where the dependence of the electric potential and the ion concentration profiles on the counterion and co-ion valences is shown. Note that, since the counterion and co-ion concentrations no longer coincide when their valences differ, only the concentration of counterions was kept at the constant value $c_1^\infty = 100$ mol/m^3.

As expected, the counterion valence has a strong bearing on the total electric charge in the $h_1 < x < h_2$ region, leading to important changes in the electric potential and ionic concentration profiles. Specifically, an increase in the counterion valence increases the counterion charge in the $h_1 < x < h_2$ region, which can lead to charge reversal even for the moderate counterion concentration considered in Figure 4a. On the contrary, the co-ion valence has a very small bearing on the electric potential since there are no co-ions in the $h_1 < x < h_2$ region, so that the small differences observed in Figure 4 are only due to dependences on the co-ion valence in the solution $h_2 < x$ region.

Finally, Figure 5 shows the dependence of the electric potential and the ion concentration profiles on the surface charge of the particle. Note that, in this figure, cations and anions exchange their roles as counterions and co-ions when the surface charge changes sign. As can be seen, the surface potential for an uncharged particle is always different from zero (positive in the considered case), and there is always a range of surface charge values for which charge reversal occurs. In the considered case (smaller minimum approach distance for cations than anions), this range extends from a zero surface charge to a negative value approximately given by eq 20. Therefore, according to the considered model, charge reversal would appear to be a common phenomenon occurring for weakly charged particles rather than an exotic one only to be expected for extremely high surface charges.

Conclusion

In this work we present a study of the equilibrium double layer surrounding charged spherical particles, considering that ions in the suspending medium have a finite size. We assume that the minimum approach distance to the particle surface is larger for co-ions than for counterions, while the distance of minimum approach between ions has the same value for both ion species. Numerical calculations made using the network simulation method and including all the features of the considered theoretical model are presented, together with rigorous analytical results valid for a flat interface and point ions in the bulk electrolyte solution.

We show that the double-layer parameters are very sensitive to the difference between the distances of minimum approach of co-ions and counterions to the particle surface: for negative particles, the potential at all points always increases with this parameter. Furthermore, and under appropriate circumstances, this increase becomes so high that the potential attains positive values leading to charge reversal. The occurrence of this phenomenon is favored by a high electrolyte concentration, high counterion valence, and low surface charge (in modulus). An analytical expression relating these parameters to the threshold value of the difference between the minimum approach distances of co-ions and counterions to the particle surface is presented.

This study shows that purely "physical" mechanisms (difference between minimum approach distances) suffice to produce charge reversal, so that these mechanisms may certainly have an important contribution to the full interpretation of this phenomenon,[37] which can also include "chemical" mechanisms such as specific ion−particle surface interactions. It shows, furthermore, that the consideration of minimum approach distance values that are independent of the surface charge is inadequate, since it predicts the occurrence of charge reversal for any set of the system parameters, provided that the absolute value of the surface charge is sufficiently low. This conclusion is to be expected, since the minimum approach distances should be determined by ion-particle surface interactions, which certainly depend on the surface charge of the particle. This dependence and its influence on the equilibrium and nonequilibrium dielectric and electrokinetic properties will be the subject of future work.

Acknowledgment. Financial support for this work by Junta de Andalucía (Project PE-2008 FQM-3993) of Spain, as well as that by CIUNT (project 26/E419) of Argentina, is gratefully acknowledged.

Appendix A

Expression 2 follows from a more general result: the Nernst−Planck equations relating the ionic fluxes, $\vec{j}_i$, with the local electric field and the ionic concentrations:

$$\vec{j}_i(\vec{r}) = -D_i c_i(\vec{r})\nabla\mu_i(\vec{r}) = -D_i c_i(\vec{r})\nabla\left\{\ln[\gamma_i(\vec{r})c_i(\vec{r})] + \frac{z_i e\phi(\vec{r})}{kT}\right\} \quad \text{(A.1)}$$

where μ_i, γ_i, and D_i are the electrochemical potential and the activity and diffusion coefficients of the ionic species i, respectively. Taking into account the spherical symmetry of the system and the condition that, in equilibrium, the ionic fluxes must vanish, transforms eq A.1 into

$$-D_i c_i(r)\frac{\mathrm{d}}{\mathrm{d}r}\left\{\ln[\gamma_i(r)c_i(r)] + \frac{z_i e\phi(r)}{kT}\right\} = 0 \quad \text{(A.2)}$$

Therefore, the electrochemical potentials must be constant throughout the system so that

$$\gamma_i(r)c_i(r)\exp\left[\frac{z_i e\phi(r)}{kT}\right] = A_i \Rightarrow c_i(r) = \frac{A_i}{\gamma_i(r)}\exp\left[-\frac{z_i e\phi(r)}{kT}\right] \quad \text{(A.3)}$$

where A_i are constants. Finally, assuming that the activity coefficients satisfy the Bikermann expression,

$$\gamma_i(r) = \gamma(r) = \frac{1}{1 - \sum_{i=1}^{m}\frac{c_i(r)}{c_i^{\max}}} \quad \text{(A.4)}$$

leads to

$$\gamma(r) = 1 + \sum_{i=1}^{m}\frac{A_i}{c_i^{\max}}\exp\left[-\frac{z_i e\phi(r)}{kT}\right] \quad \text{(A.5)}$$

Using this result together with

$$K_i = \frac{A_i}{1 + \sum_{i=1}^{m}\frac{A_i}{c_i^{\max}}} \quad \text{(A.6)}$$

transforms eq A.3 into eq 2.

On the other hand, from eq A.2 and in order to ensure equilibrium between the different regions, the electrochemical potential of each ionic species must be continuous at the boundaries between the different regions:

$$\mu_i((a + h_{i+1})^-) = \mu_i((a + h_{i+1})^+) \quad \forall i \in (1, 2, ..., m - 1) \quad \text{(A.7)}$$

Taking into account that the electric potential must be continuous at these same boundaries, expression A.7 simplifies to

$$\ln\left[\frac{\gamma((a + h_{i+1})^+)c_i((a + h_{i+1})^+)}{\gamma((a + h_{i+1})^-)c_i((a + h_{i+1})^-)}\right] = \ln\left(\frac{K_i^+}{K_i^-}\right) = 0 \Rightarrow K_i^+ = K_i^- \quad \text{(A.8)}$$

where eq A.3 was used.

Finally, using eq A.8 and recalling that, in the solution region, $r > a + h_m$, the K_i constants coincide with the corresponding bulk ion concentrations, leads to

$$K_i = \begin{cases} 0 & a < r < a + h_i \\ c_i^{\infty} & a + h_i < r \end{cases} \quad \text{(A.9)}$$

Appendix B

The generalized Poisson eq 13 written in terms of the dimensionless potential and considering just two ion species in the electrolyte solution is

$$\frac{d^2y(x)}{dx^2} + \frac{2}{x+a}\frac{dy(x)}{dx} = -\frac{\kappa^2}{{z_1}^2c_1^\infty + {z_2}^2c_2^\infty} \times \frac{z_1c_1^\infty e^{-z_1y} + z_2c_2^\infty e^{-z_2y}}{1 + \frac{c_1^\infty}{c_1^{max}}(e^{-z_1y} - 1) + \frac{c_2^\infty}{c_2^{max}}(e^{-z_2y} - 1)} \quad \text{(B.1)}$$

where

$$\kappa = \sqrt{\frac{z_1e^2N_Ac_1^\infty(z_1 - z_2)}{kT\varepsilon_e}}$$

in view of the condition of electroneutrality far from the particle:

$$z_1c_1^\infty + z_2c_2^\infty = 0$$

Analytical solutions only exist for point ions ($c_i^{max} \to \infty$) and a flat interface ($a \to \infty$). Under these conditions, the equation to be solved reduces to

$$\frac{d^2y}{dx^2} = -\frac{\kappa^2}{z_1 - z_2}(e^{-z_1y} - e^{-z_2y}) \quad \text{(B.2)}$$

External Region $h_2 < x$

The full eq B.2 that can be written as

$$d\left(\frac{dy}{dx}\right)^2 = -\frac{2\kappa^2}{z_1 - z_2}(e^{-z_1y} - e^{-z_2y})\,dy$$

must be solved. Integrating this expression from a generic point to infinity (where $dy/dx = 0$),

$$\left(\frac{dy}{dx}\right)^2 = \frac{2\kappa^2}{z_1 - z_2}\left(\frac{e^{-z_1y} - 1}{z_1} - \frac{e^{-z_2y} - 1}{z_2}\right) \quad \text{(B.3)}$$

and taking into account that the sign of y is opposite the sign of dy/dx, leads to

$$\frac{dy}{dx} = -\text{sign}(y)\kappa\sqrt{\frac{2}{z_1 - z_2}\left(\frac{e^{-z_1y} - 1}{z_1} - \frac{e^{-z_2y} - 1}{z_2}\right)} \quad \text{(B.4)}$$

This equation can be integrated from $x = h_2$ to a generic point. However, analytic results can only be obtained for the following three cases:[38]

(a) For $z_1 = -z_2 = z$:

$$y = \frac{2}{z}\ln\frac{(e^{zy_2/2} + 1)e^{\kappa x} + (e^{zy_2/2} - 1)e^{\kappa h_2}}{(e^{zy_2/2} + 1)e^{\kappa x} - (e^{zy_2/2} - 1)e^{\kappa h_2}}$$

(b) For $z_1 = -2z_2 = 2z$:

$$y = \frac{1}{z}\ln\frac{3\left[\frac{(\sqrt{2e^{zy_2} + 1} + \sqrt{3})e^{\kappa x} + (\sqrt{2e^{zy_2} + 1} - \sqrt{3})e^{\kappa h_2}}{(\sqrt{2e^{zy_2} + 1} + \sqrt{3})e^{\kappa x} - (\sqrt{2e^{zy_2} + 1} - \sqrt{3})e^{\kappa h_2}}\right]^2 - 1}{2}$$

(c) For $2z_1 = -z_2 = 2z$:

$$y = -\frac{1}{z}\ln\frac{3\left[\frac{(\sqrt{1 + 2e^{-zy_2}} + \sqrt{3})e^{\kappa x} + (\sqrt{1 + 2e^{-zy_2}} - \sqrt{3})e^{\kappa h_2}}{(\sqrt{1 + 2e^{-zy_2}} + \sqrt{3})e^{\kappa x} - (\sqrt{1 + 2e^{-zy_2}} - \sqrt{3})e^{\kappa h_2}}\right]^2 - 1}{2}$$

where $y_2 = y(x = h_2)$.

Intermediate Region $h_1 < x < h_2$

The equation to be solved reduces to

$$d\left(\frac{dy}{dx}\right)^2 = -\frac{2\kappa^2}{z_1 - z_2}e^{-z_1y}\,dy$$

Integrating this expression from a generic point to $x = h_2$,

$$\left(\frac{dy}{dx}\bigg|_{h_2}\right)^2 - \left(\frac{dy}{dx}\right)^2 = \frac{2\kappa^2}{z_1(z_1 - z_2)}(e^{-z_1y_2} - e^{-z_1y})$$

and using eq B.3 together with the continuity of the electric displacement at $x = h_2$ condition, gives

$$\frac{dy}{dx} = -\text{sign}(y_2)\kappa\sqrt{\frac{2}{z_1(z_1 - z_2)}}\sqrt{e^{-z_1y} - \frac{z_1e^{-z_2y_2} - z_1 + z_2}{z_2}} \quad \text{(B.5)}$$

Integrating this expression from a generic point to $x = h_2$, leads to two possible solutions:

(a) For $\beta^2 = (z_1e^{-z_2y_2} - z_1 + z_2)/z_2 > 0$

$$y = \frac{2}{z_1}\ln\left\{\frac{1}{\beta}\sin\left[\sin^{-1}(\beta e^{z_1y_2/2}) + \text{sign}(y_2)\kappa\beta\sqrt{\frac{2z_1}{z_1 - z_2}}\frac{h_2 - x}{2}\right]\right\} \quad \text{(B.6)}$$

(b) For $\beta^2 = -(z_1e^{-z_2y_2} - z_1 + z_2)/z_2 > 0$

$$y = \frac{2}{z_1}\ln\left\{\frac{1}{2\beta}\left[\frac{\exp\left(\mathrm{sign}(y_2)\kappa\beta\sqrt{\frac{2z_1}{z_1 - z_2}}\frac{h_2 - x}{2}\right)}{\sqrt{\beta^2 e^{z_1 y_2} + 1} - \beta e^{z_1 y_2/2}} - \frac{\sqrt{\beta^2 e^{z_1 y_2} + 1} - \beta e^{z_1 y_2/2}}{\exp\left(\mathrm{sign}(y_2)\kappa\beta\sqrt{\frac{2z_1}{z_1 - z_2}}\frac{h_2 - x}{2}\right)}\right]\right\}$$

Internal Region $0 < x < h_1$

The expression to be solved reduces to the Laplace equation:

$$\frac{d^2 y}{dx^2} = 0$$

that has the solution

$$y = y_0 + \alpha x$$

The value of α is determined by eq B.5 together with the condition of continuity of the electric displacement at $x = h_1$.

$$\frac{dy}{dx} = -\mathrm{sign}(y_2)\kappa\sqrt{\frac{2}{z_1(z_1 - z_2)}}\sqrt{e^{-z_1 y} - \frac{z_1 e^{-z_2 y_2} - z_1 + z_2}{z_2}}$$

(a) For $\beta^2 = (z_1 e^{-z_2 y_2} - z_1 + z_2)/z_2 > 0$. The sign of the derivative can be determined calculating the value of the coordinate $x = x_m$ for which the derivative vanishes and changes sign while y attains a maximum value y_m:

$$e^{-z_1 y_m} - \beta^2 = 0$$

which leads to

$$x_m = h_2 - 2\,\mathrm{sign}(y_2)\sqrt{\frac{z_1 - z_2}{2z_1}}\frac{\sin^{-1}(1) - \sin^{-1}(\beta e^{z_1 y_2/2})}{\kappa\beta}$$

If x_m is less than h_1, the derivative does not change sign between h_1 and h_2 so that

$$\alpha = -\mathrm{sign}(y_2)\kappa\sqrt{\frac{2}{z_1(z_1 - z_2)}}\sqrt{e^{-z_1 y_1} - \beta^2} \quad \text{(B.7)}$$

If x_m is between h_1 and h_2, the derivative changes sign between h_1 and h_2 so that

$$\alpha = \mathrm{sign}(y_2)\kappa\sqrt{\frac{2}{z_1(z_1 - z_2)}}\sqrt{e^{-z_1 y_1} - \beta^2}$$

(b) For $\beta^2 = -(z_1 e^{-z_2 y_2} - z_1 + z_2)/z_2 > 0$. In the above expressions, $y_1 = y(h_1)$.

$$\alpha = -\mathrm{sign}(y_2)\kappa\sqrt{\frac{2}{z_1(z_1 - z_2)}}\sqrt{e^{-z_1 y_1} + \beta^2}$$

Finally, the surface potential is determined by the continuity of the electric potential at $x = h_1$:

$$y_0 = y_1 - \alpha h_1$$

while the surface charge is determined by the discontinuity of the electric displacement at $x = 0$:

$$\sigma_s = -\alpha kT\varepsilon_e/e$$

Condition for Charge Reversal

Charge reversal occurs for a limited range of surface charge values. The upper limit of this range is clearly zero: for positive surface charges, the potential is positive for all distances. As for the lower limit, it is determined by the condition that the potential y_2 vanishes since, for smaller surface charges, the potential is negative for all distances.

For $y_2 = 0$, condition (a) in the intermediate region is always satisfied so that

$$\beta^2 = (z_1 e^{-z_2 y_2} - z_1 + z_2)/z_2 = 1$$

Therefore, using eq B.6,

$$y_1 = \frac{2}{z_1}\ln\left[\cos\left(\kappa\sqrt{\frac{2z_1}{z_1 - z_2}}\frac{h_2 - h_1}{2}\right)\right]$$

which, combined with eq B.7, leads to the following condition for charge reversal:

$$0 < \alpha < \kappa\sqrt{\frac{2}{z_1(z_1 - z_2)}}\tan\left(\kappa\sqrt{\frac{2z_1}{z_1 - z_2}}\frac{h_2 - h_1}{2}\right)$$

or

$$h_2 - h_1 > \frac{1}{z_1 e}\sqrt{\frac{2kT\varepsilon_e}{c_1^\infty N_A}}\tan^{-1}\sqrt{\frac{\sigma_s^2}{2kT\varepsilon_e c_1^\infty N_A}}$$

It should be noted that these last results are valid for all values of the valences z_1 and z_2. This happens because the restrictions $z_1 = -z_2$, $z_1 = -2z_2$, or $2z_1 = -z_2$ only apply to the existence of an analytical expression for the potential in the external region. On the contrary, the calculation of the potential in the intermediate and internal regions only requires an analytical expression for the derivative dy/dx, which is available for all valence values (eq B.4).

References and Notes

(1) Russel, W. B.; Saville, D. A. Schowalter, W. R. *Colloidal Dispersions*; Cambridge University Press: Cambridge, 1995.

(2) Hunter, R. J. *Foundations of Colloid Science*; Oxford University Press: London, 1995; Vol. I.

(3) Lyklema, J. *Fundamentals of Colloid and Interface Science: Vol II, Solid/Liquid Interfaces*; Academic Press: London, 1995.

(4) Bikerman, J. J. Structure and Capacity of Electrical Double Layer. *Philos. Mag.* **1942**, *33*, 384.

(5) Brodowsky, H.; Strehlow, H. Zur Strucktur der Elektrochemischen Doppelschicht. *Z. Elektrochem.* **1959**, *63*, 262.

(6) Wicke, E.; Eigen, M. 'Uber den Einfluss des Raumbedarfs von Ionen in Wassriger Losung auf Ihre Verteilung im Elektrischen Feld und Ihre Aktivitatskoeffizienten. *Z. Elektrochem.* **1952**, *56*, 551.

(7) Levine, S.; Bell, G. M. Modified Poisson-Boltzmann and Free Energy of Electrical Double Layers in Hydrophobic Colloids. *Discuss Faraday Soc.* **1966**, *42*, 69.

(8) Ruckenstein, E.; Schiby, D. Effect of the Excluded Volume of the Hydrated Ions on Double-Layer Forces. *Langmuir* **1985**, *1*, 612.

(9) Chodanowski, P.; Stoll, S. Polyelectrolyte Adsorption on Charged Particles: Ionic Concentration and Particle Size Effects - A Monte Carlo Approach. *J. Chem. Phys.* **2001**, *115* (10), 4951.

(10) Jimenez-Angeles, F.; Lozada-Cassou, M. A Model Macroion Solution Next to a Charged Wall: Overcharging, Charge Reversal, and Charge Inversion by Macroions. *J. Phys. Chem. B* **2004**, *108*, 7286.

(11) Diehl, A. Smoluchowski Equation and the Colloidal Charge Reversal. *J. Chem. Phys.* **2006**, *125*, 054902.

(12) Jimenez-Angeles, F.; Lozada-Cassou, M. On the Regimes of Charge Reversal. *J. Chem. Phys.* **2008**, *128*, 174701.

(13) Diehl, A.; Levin, Y. Colloidal Charge Reversal: Dependence on the Ionic Size and the Electolyte Concentration. *J. Chem. Phys.* **2008**, *129*, 124506.

(14) Martin-Molina, A.; Rodriguez-Beas, C.; Hidalgo-Alvarez, R.; Quesada-Perez, M. Effect of Surface Charge on Colloidal Charge Reversal. *J. Phys. Chem. B* **2009**, *113*, 6834.

(15) Ibarra-Armenta, J. G.; Martín-Molina, A.; Quesada-Pérez, M. Testing a Modified Model of the Poisson-Boltzmann Theory that Includes Ion Size Effects through Monte Carlo Simulations. *Phys. Chem. Chem. Phys.* **2009**, *11*, 309.

(16) Adamczyk, Z.; Warszysnky, P. Role of Electrostatic Interactions in Particle Adsorption. *Adv. Colloid Interface Sci.* **1996**, *63*, 41.

(17) Woelki, S.; Kohler, H. H. A Modified Poisson-Boltzmann Equation. I. Basic Relations. *Chem. Phys.* **2000**, *261*, 411.

(18) Borukhov, I.; Andelman, D.; Orland, H. Adsorption of Large Ions from a Electrolyte Solution. *Electrochim. Acta* **2000**, *46*, 221.

(19) Bohinc, K.; Kralj-Iglic, V.; Iglic, A. Thickness of Electrical Double Layer. Effect of Ion Size. *Electrochim. Acta* **2001**, *46*, 3033.

(20) Hsu, J. P.; Jiang, J. M.; Tseng, S. J. Estimation of the Ionic Distribution in a Reverse Micelle: Effect of Ionic Size. *J. Phys. Chem. B* **2003**, *107*, 14429.

(21) Yu, J.; Aguilar-Pineda, G. E.; Antillón, A.; Dong, S. H.; Lozada-Cassou, M. The Effects of Unequal Ionic Sizes for an Electrolyte in Charged Slit. *J. Colloid Interface Sci.* **2006**, *295*, 124.

(22) Biesheuvel, P. M.; van Soestbergen, M. Counterion Effects in Mixed Electrical Double Layers. *J. Colloid Interface Sci.* **2007**, *316*, 490.

(23) Kilic, M. S.; Bazant, M. Z.; Ajdari, A. Steric Effects in the Dynamics of Electrolytes at Large Applied Voltages. II. Modified Poisson−Nernst Planck Equations. *Phys. Rev. E* **2007**, *75*, 021503.

(24) López-García, J. J.; Aranda-Rascón, M. J.; Horno, J. Electrical Double Layer around a Spherical Colloid Particle: The Excluded Volume Effect. *J. Colloid Interface Sci.* **2007**, *316*, 196.

(25) López-García, J. J.; Aranda-Rascón, M. J.; Horno, J. Excluded Volume Effect on the Electrophoretic Mobility of Colloidal Particles. *J. Colloid Interface Sci.* **2008**, *323*, 146.

(26) Aranda-Rascón, M. J.; Grosse, C.; López-García, J. J.; Horno, J. Electrokinetics of Suspended Charged Particles Taking into Account the Excluded Volume Effect. *J. Colloid Interface Sci.* **2009**, *335*, 250.

(27) Aranda-Rascón, M. J.; Grosse, C.; López-García, J. J.; Horno, J. Influence of the Finite Ion Size on the Predictions of the Standard Electrokinetic Model: Frequency Response. *J. Colloid Interface Sci.* **2009**, *336*, 857.

(28) Bhuiyan, L. B.; Outhwaite, C. W. Comparison of Exclusion Volume Corrections to the Poisson−Boltzmann Equation for Inhomogeneous Electrolytes. *J. Colloid Interface Sci.* **2009**, *331*, 543.

(29) Bazant, M. Z.; Kilic, M. S.; Storey, B. D.; Ajdari, A. Towards an Understanding of Induced-Charge Electrokinetics at Large Applied Voltages in Concentrated Solutions. *Adv. Colloid Interface Sci.* **2009**, *152*, 48.

(30) Grahame, D. C. The Electrical Double Layer and the Theory of Electrocapillarity. *Chem. Rev.* **1947**, *41*, 441.

(31) López-García, J. J.; Moya, A. A.; Horno, J.; Delgado, A.; González-Caballero, F. A Network Model of the Electrical Double Layer around a Colloid Particle. *J. Colloid Interface Sci.* **1996**, *183*, 124.

(32) López-García, J. J.; Horno, J.; Grosse, C. Numerical Solution of the Poisson−Boltzmann Equation for Suspended Charged Particles Surrounded by a Charged Permeable Membrane. *Phys. Chem. Chem. Phys.* **2001**, *3*, 3754.

(33) López-García, J. J., Horno, J. In *Network Simulation Method*; Horno, J., Ed.; Research Signpost: Trivandrum, India, 2002.

(34) Tang, Z.; Scriven, L. E.; Davis, H. T. A Three Component Model of the Electrical Double Layer. *J. Chem. Phys.* **1992**, *97*, 494.

(35) Antypov, D.; Barbosa, M. C.; Holm, C. Incorporation of Excluded Volume Correlations into Poisson−Boltzmann Theory. *Phys. Rev. E* **2005**, *71*, 061106.

(36) Nightingale, E. R. Phenomenological Theory of Ion Solvation. Effective Radii. *J. Phys. Chem.* **1959**, *63*, 1381.

(37) Lyklema, J. Quest for Ion−Ion Correlations in Electric Double Layers and Overcharging Phenomena. *Adv. Colloid Interface Sci.* **2009**, *147*, 205.

(38) Grosse, C. Generalization of a Classic Thin Double Layer Polarization Theory of Colloidal Suspensions to Electrolyte Solutions with Different Ion Valences. *J. Phys. Chem. B* **2009**, *113*, 8911.

JP9122369